A biophysically realistic Model of the Retina

Melissa Louey
Department of Mechanical Engineering
The University of Melbourne
Melbourne, VIC 3010
mlouey@student.unimelb.edu

Piotr Sokół
Social and Psychological Sciences
University College Utrecht
Utrecht, Elmarelaan 37
piotr.a.sokol@gmail.com

Abstract

The intricate neural circuit in the retina is responsible for detecting and converting light into electrical signal. Basic imaging processing occurs within the network. This paper analysed the convergence of information within the retina at a cellular level. It found significant non-linear behaviour at the amacrine level. Possible accounts for this phenomenon have been presented.

1 Introduction

The retina, a tissue located at the back of the eye, is responsible for detecting and converting light into electrical signals where it can be sent to the brain for the majority of the image processing[1]. However, a small portion of image processing already occurs within the retina due to the neural circuitry developed in the eye. In order to understand the processing within the retina, several computational models mimicking the characteristics of each cell type have been produced[1], [2]. Using these computational models, it is possible to investigate and predict biological phenomena leading to greater understanding of the intricacies of the human eye.

To generate a computational model of the retina, it is necessary to develop an understanding of the anatomy and physiology in the eye.

1.1 Physiology of the Eye

The retina is built up of three distinct layers. Each layer is composed of distinct cell types that are linked together in an intricate network to relay signals to the optic nerve.

The first layer is primarily composed of light receptors, known as photoreceptors. These are located at the back of the retina and respond to light stimulus, converting information into an electrical signal. There are two basic forms of photoreceptors. Rods are highly responsive to low light and only respond to black and white colours. These are mainly located in the peripheral regions of the human eye. Meanwhile, three types of cones exists, each detecting a specific colour given sufficient light; blue, green or red. Cones are concentrated in the central region of the retina known as the macula. It should be noted that photoreceptors are characterised to have consistent tonic neural spiking with no light input, and displays a hyperpolarisation during stimulation (figure 1).

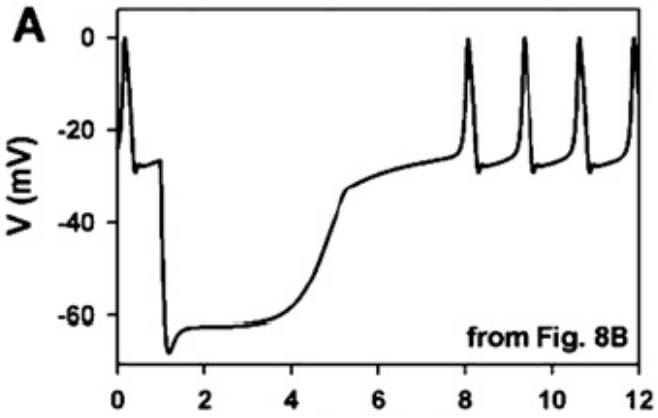

Figure 1: Membrane voltage of a photoreceptor. Light stimulus is presented between 1 and 5 milliseconds and displays a hyperpolarisation. Otherwise, tonic spiking is displayed[3].

The second layer, known as the inner nuclear layer is composed of a myriad of cells, each with several subclasses. In the human eye, cells including horizontal cells, bipolar cells and amacrine cells exist within this layer. The final layer is composed of ganglion cells which bundle information from bipolar and amacrine cells to create the optic nerve. Neural synapses between these three layers also have distinct properties and are known as the outer and inner plexiform layer. The anatomical representation of the retina is displayed in figure 2.

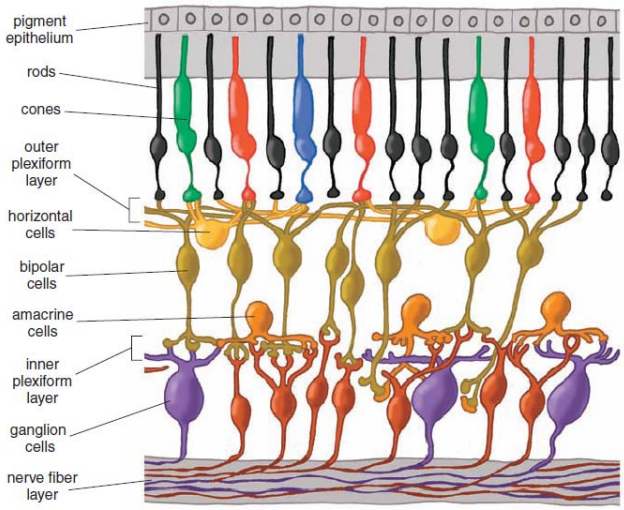

Figure 2: Different cells within the retina are connected in a specific manner and forms three discrete layers. Light enters the eye, making its way to the photoreceptors, rods and cones, located at the back of the eye.

1.3 Objectives

In this paper, a basic neural model of is created and its characteristics

investigated. In particular, the behaviour of each cell type is analysed and the performance of the model is explored against sample images.

2 Method

2.1 Modelling the Retina

The model of the retina was generated using NEURON software with each cell type represented as a single compartmental Hodgkin-Huxley neuron with various ion channels. Since the retina is a highly intricate network of neurons, several cell types were omitted from the modelling process. Instead, a basic construct was developed.

In the model created, four general cell types were included; rods, bipolar cells, amacrine II cells and ganglion cells. The ratio of cell types between each retinal layer was based on the fovea in a cat. It has been determined that cats synapse 15 rods to one bipolar cell; 20 bipolar cells to one amacrine II cell and four amacrine cell to a single ganglion [4]. Due to the computational constraints, the model was scaled and reduced to exhibit 4 rods per bipolar cell, four bipolar cells synapsing with a single amacrine II cell, which connects to a single ganglion. A schematic of the model is shown in figure 3.

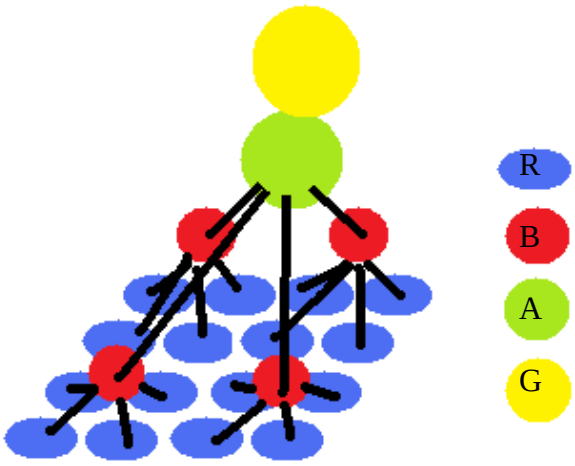

Figure 3: A schematic of the retinal model and cell type connections. 4 rods (R) synapse with each bipolar cell (B). 4 bipolar cells connect to a single amacrine II cell (A) which synapses directly to a ganglion cell (G).

Each cell type was loosely based on the Hodgekin-Huxley model of neuronal input and was collated from two previous modelling attempts by Kourennyi, et al[3] and Publio et al[2]. Kourennyi, et al [3] produced a computational model for rods that encompassed calcium channels, non-inactivating potassium channels, nonselective cation H+ channels and delayed rectifier-like potassium channels. The work of Publio [2]was used to generate models of bipolar, amacrine II and ganglion cells and incorporated several ionic channels. The bipolar included the following channels in addition to the HH channels: L-type calcium channels, hyperpolarization activated nonselective cation channel, delayed rectifying potassium channel[5], [2]. The neurons were modelled in accordance with the realistic biophysical data, however

they were reduced to single compartment models for lack of topographical data. Moreover, the use of specific topographic data would not significantly alter the expected firing in the ganglia, hence the point process approximation is sufficient.

The connectivity between each cell type was further determined to have a graded synaptic input [2].The spatial orientation of the rods synapsing to each particular bipolar cell was based on the biological phenomenon normally observed in nature. Spatially, photoreceptors on the retina receive input in a similar layout as the stimulus presented and clusters of rods a synapse with a single bipolar cell[6]. As a result, the model developed had a grid of two by two rods synapsing with a ganglion cell. This network provided the basis of our retina network.

2.2 Image Analysis

The model generated was used to analyse arbitrary images to test the performance of the network. Each photoreceptor was presented with the light intensity of one pixel on a gray scale image (Figure 4). Since four rods synapsed to a single bipolar and four bipolar cells injected current into a single amacrineII cell, the convergence of the network lead to a low resolution output image. Consequentially, the retina output was a sixteenth of the size of the stimulus image.

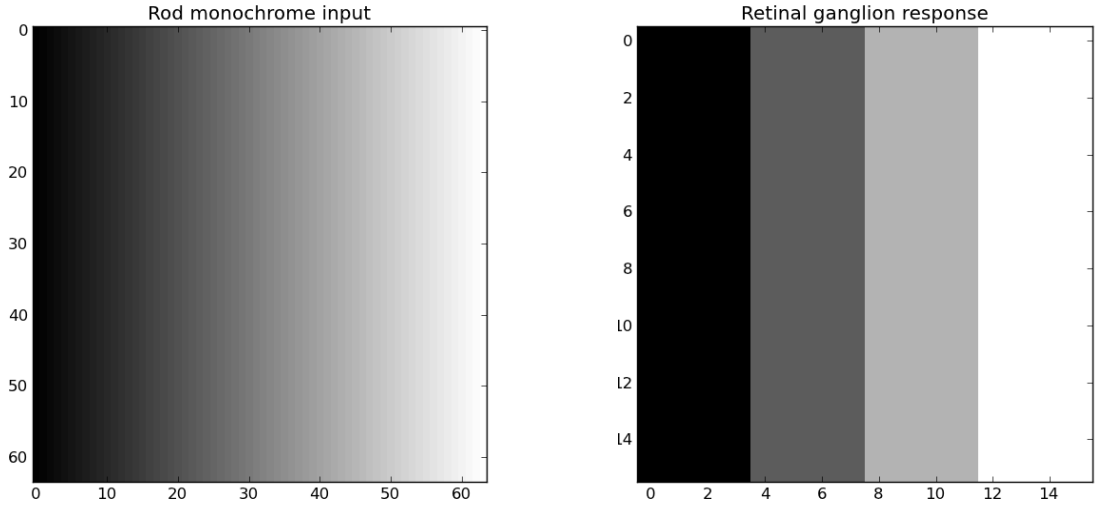

Figure 4: Sample input stimulus presented to the retina model and its interpretation of the image. Notice the increased level of pixilation due to the convergence on information from 64 rods into 4 ganglion cells.

Input light intensity of the image was scaled to involve intensities between a specified range to ensure injected current into photoreceptors resulted in ganglions spiking at a rate inversely proportional to injected current. That is, as light intensity increased or appeared whiter, the ganglion spiking frequency decreased. Outside of these bounds, ganglion cells do not exhibit this behaviour and is a limitation of the model used. Spiking frequency was assumed to be a linear function of injected current. For a given input, the maximum spiking frequency was mapped to black, whilst the minimum spiking frequency was mapped to white.

4 Results and analysis

To establish the correct physiological rate of firing of a ganglion cell we stimulated the cell with different currents, while remembering that the rod responses to same stimuli have to be constrained to a biologically realistic range of membrane voltages. The range of current, as proposed by Attwell et al. [7] suggest that the range of stimulation should be a linear scaling between 0 and -50 pA, the latter value corresponding to an increase in photostimulation. When stimulated with the aforesaid ranges we found an inverse relationship between the magnitude of the current and the firing rate. At current near 0pA, the ganglion had a spiking rate of approximately 145Hz, while at 50pA the ganglion did not spike. As a further step we attempted to extend the simulation to a 2x2 ganglion network. The initial test applied to the network consisted of the application of a uniform stimulus, to check consistency findings for the 1 ganglion network. However, at this level, the stimulation with a uniform field has resulted in different spiking rates for different ganglia. Below, a matrix representation of the spiking rates of the retinal ganglia in hertz (Hz).

$$\begin{matrix} 42.68 & 62.84 \\ 67.48 & 68.15 \end{matrix}$$

When comparing the obtained values with the values from the previous simulation which consisted of only one ganglion, we noticed that only the value (1,1) in the matrix is the equal to that obtained in the previous simulation. The disparity between the values, which were expected to be equal, is depicted in figure 5. Instead of obtaining two uniform images, the output image was tiled with different intensities.

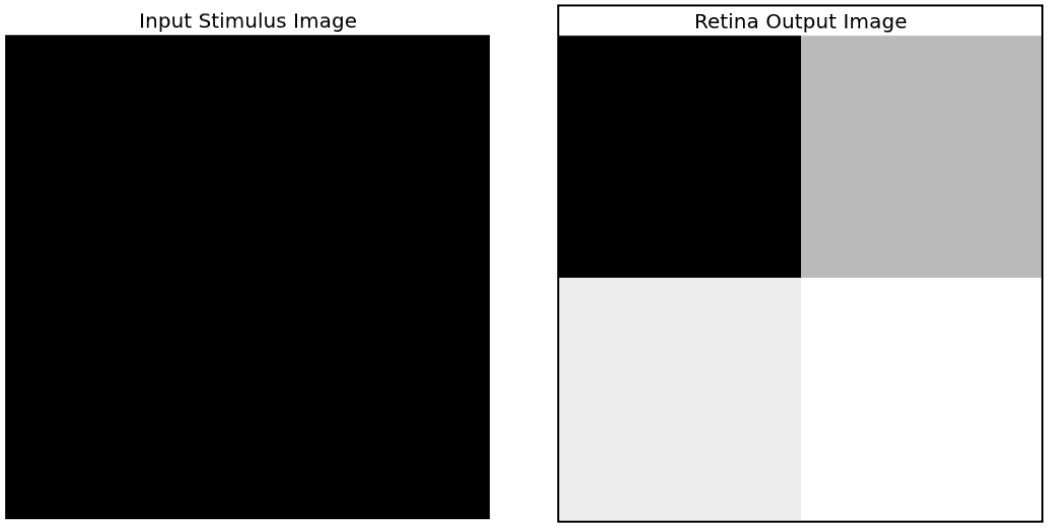

Figure 5: The input does not match the output; the predicted color of the output was uniform, in reflection of the equal stimulation of all rods, in the first layer of the model.

To find the source of error, electrical activity has been recorded at each level of the model. The simulated values for each level are presented below.

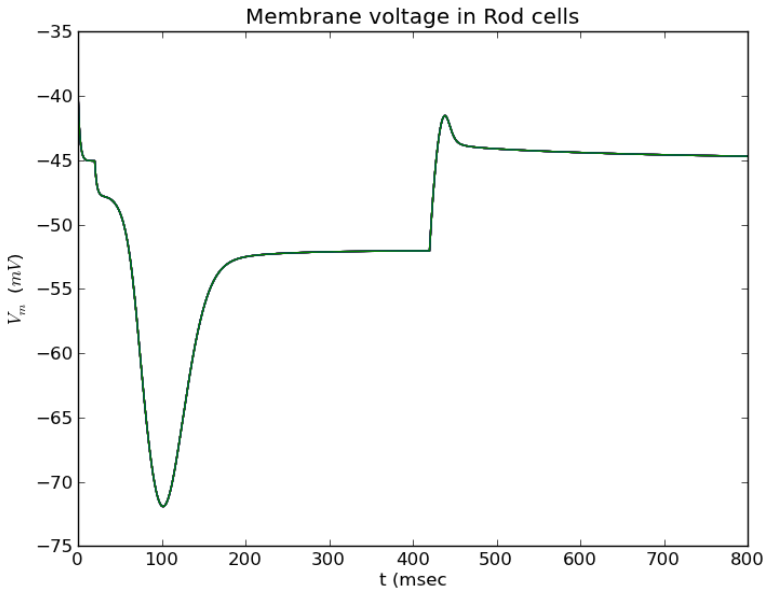

Figure 6: To find the malfunctioning part of the code, the recordings were first taken from the rod cells. However, as seen in graph, all of the 16 rod cells show consistent responses to the stimuli. All of the 16 cells were overlaid on top of each other, and the presence of one curve indicates that all of the rod responses were identical.

The results found in figure four implicate that the disparity is not a result of problems wiring the stimuli to the rods or the method used to calculate the rod responses. The membrane potential is within biophysical ranges and the shape of the curve is similar to that found in data recorded from real cells. For a comparison with such data see **Appendix 1.** The stimulus mimicking injected current is applied only at 20 miliseconds. In response to the injected current, the cell hyperpolarizes rapidly and reaches a minimal membrane potential of approximately -70mV. The prolonged exposure to the stimulus causes a depolarization; this depolarization can be seen for t>200msec. The injected current is stopped after 400 miliseconds. This corresponds to a rapid depolarization of the cell accompanied by a transient overshoot of the resting potential.

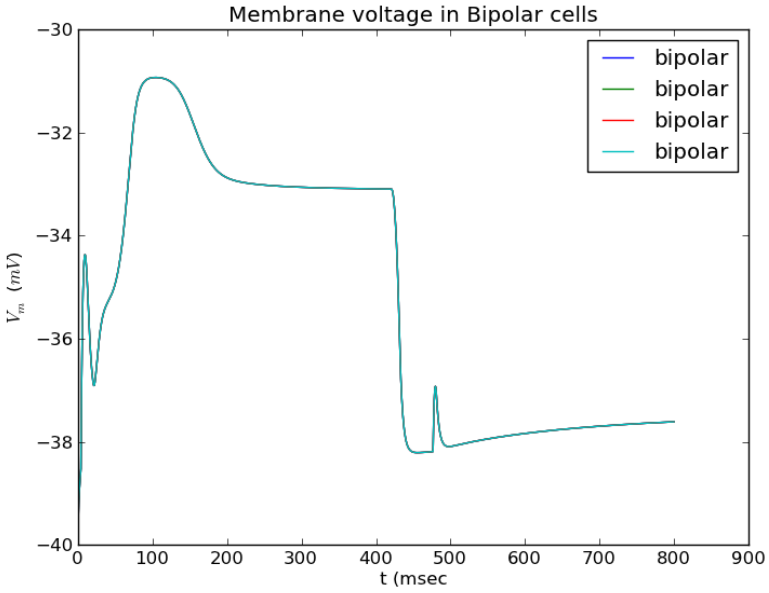

Figure 7: The next level of the model was solely composed of bipolar cells. There was a 4:1 convergence at the rod-bipolar synapse and hence, given that the rod layer was composed of 16 cells, the rod layer is composed of only 4 cells. Again, the cells exhibit highly consistent responses to the equal stimulation of the rods. All 4 lines tracing the voltage are superimposed, and there are no visible divergences from one another.

The data shown in figure 7 indicates that the network is fully functional up to the bipolar layer. No difference was found in electrophysiological responses of the cells, which could later cause different spiking rates in the optic ganglia. Notably the membrane potential and its time course are consistent with simulations obtained from Publio et al.[2] and with electrophysiological data, as seen in **Appendix 1**. The initial variation in membrane voltage, as seen for t<20 msec, results from the delay in stimulus application. The stimulus current is injected only after 20 miliseconds and lasts for 400 miliseconds. Given that the synapses are graded, the stimulus does not have to elicit an action potential to cause synaptic transmission. The type of synaptic connectivity also accounts for the activity seen for t>400msec. After the stimulus has ended, the rod cell depolarizes to its resting potential. However, just before the membrane potential tapers off to the resting potential, there is a surge in the rod membrane potential. The surge in membrane potential reflects the depolarization overshoot in the rods.

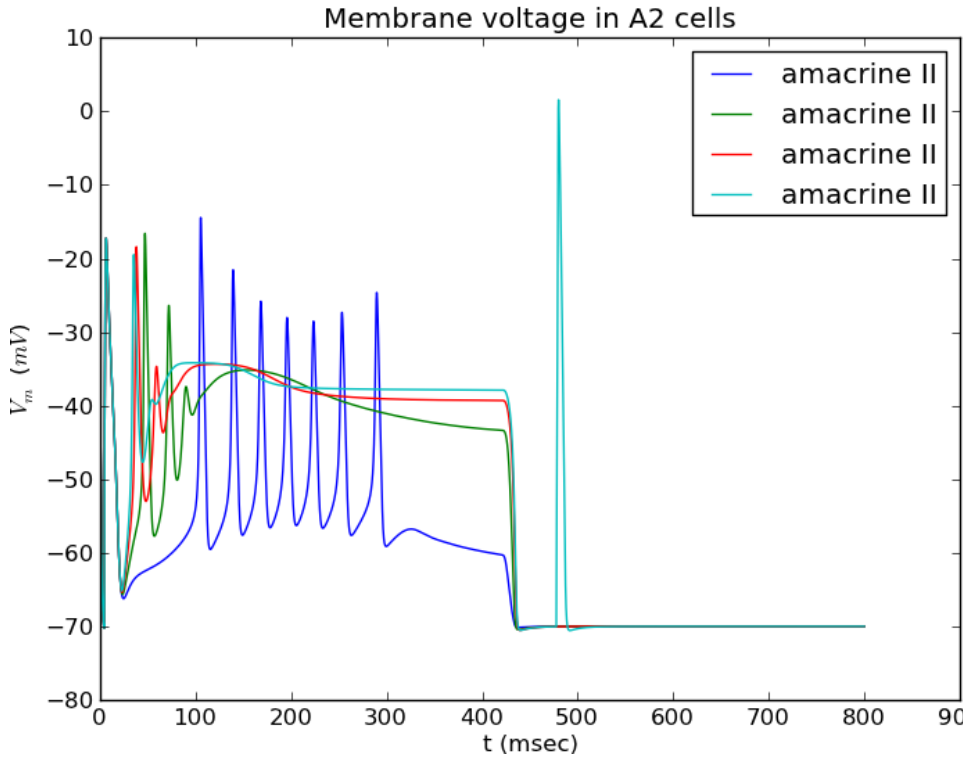

Figure 8: This level represents the activity of amacrine cells. Each of these cells is connected to one bipolar and one ganglion, as delineated in the practical considerations underlying this model. The amacrine cells take identical input from the bipolar cells; however, there is no consistency in their outputs. The amacrine differ from one another in membrane potentials, as seen in the figure.

The amacrine cell activity cannot be easily reconciled with the inputs, given that the their inputs are identical. This disparity between afferent and efferent potentials points to their role in the erroneous computation of the ganglion firing rates. There are several possibilities that could account for these incorrect results. One possibility includes incorrect connections between bipolar cells and amacrine

cells. Another possibility is that the graded synapses that connect amacrine and bipolar cells interact in non-linear ways. We tested this possibility, assuming a stochastic component to either the neurons (random start-up) or the synapses. The data obtained from several iterations was identical, indicating that there were stochastic effects. This points to specific connection problem, however, the same procedures were applied to all the synaptic connections, and thereby we should see similar disparities at all other synapses. The synapse could not be replaced with prepackaged Neuron synapses, because the graded nature of the synapse is critical to the fidelity of the model. The substitution of the synapse would result in behavior vastly different from the one exhibited by real cells. The final figures show a comparison of ganglia spiking as a response to amacrine signalling. The different behaviour is transmitted to this level. The chaotic behaviour cannot be accounted for otherwise than connection abnormalities, however the use of the same synaptic algorithms should have resulted in equal synaptic outputs.

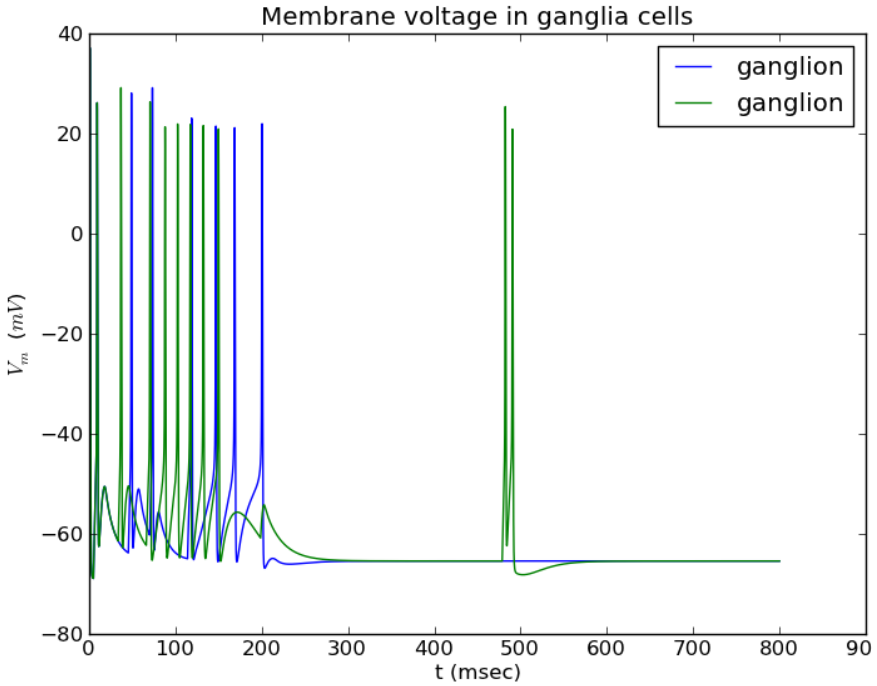

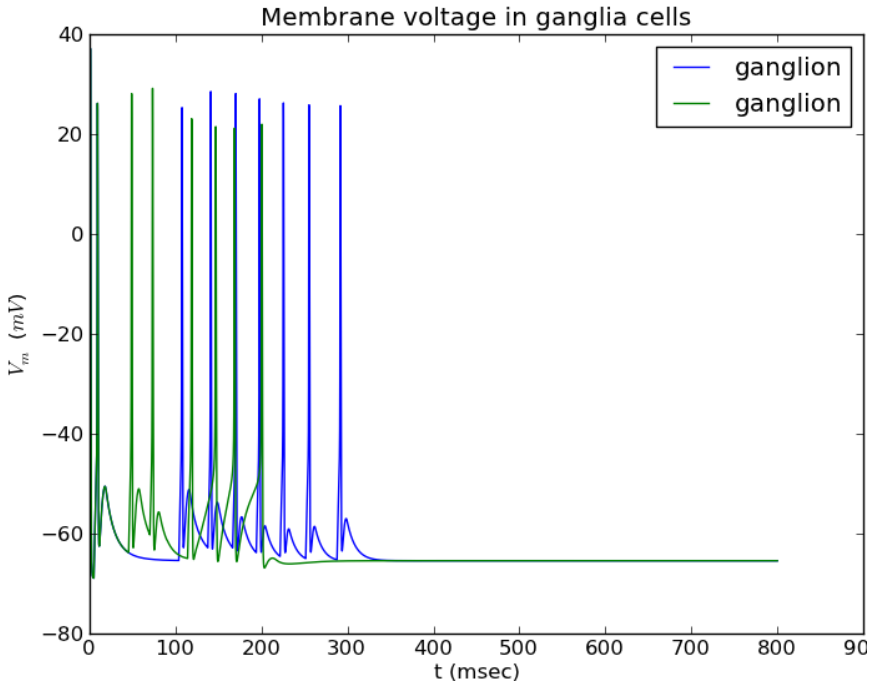

Figure 8: The ganglion spiking reflects the significant impact of the disparity of the amacrine membrane potentials. The plots were split up into arbitrarily chosen ganglia to avoid crowding in the left end of both plots. All four cells exhibit most activity within the first 300 msec, which might correspond to the big hyperpolarization of the rods. It is not necessarily so, due to the fact that all of the cells seem to cluster at left end of the plots. If the spiking was caused by rod hyperpolarizaiton, then we would see a significant difference between the activity at t<20msec and t>20msec, that is after the onset of the stimulus. Despite disparity between the cells, the range of values as well as the general spiking behaviour follows predicitions[1], [8].

The non-linear or erroneous effects from the amacrine level transfer to this level resulting in incorrect spiking frequencies. As said, a general tendency for spikes to cluster at low t values can be observed; however apart from this the cells behave in a chaotic manner.

7 Future Work

This computational network model of the model has the potential to be continually remodelled to incorporate different physiological and biological aspects of the retina. In this paper, a relatively simple representation of the retina was constructed that only encompassed the four major cell types. It is hoped that in the future, the network itself can include a variety of types for each given cell type as well as introducing new cells types such as horizontal cells.

Further, rods have been reported to be inter-connected with their neighbouring cells by virtue of gap junctions[2]. These connections impact the response of neighbouring rods and will affect the retinal interpretation of the stimulus. The integration of these features will facilitate the development of a closer representation of the biological eye.

Acknowledgments

We would like to acknowledge and thank Professor Gert Cauwenberghs and Jeffery Banks for all their assistance, feedback and contributions in constructing and implementing the retina model.

References

[1] H. Kolb, “How the Retina Works Much of the construction of an image takes place in the retina itself through the use of specialized neural circuits,” *American Scientist*, vol. 91, no. 1, pp. 28–35, 2003.

[2] R. Publio, R. F. Oliveira, and A. C. Roque, “A Computational Study on the Role of Gap Junctions and Rod Ih Conductance in the Enhancement of the Dynamic Range of the Retina,” *PLoS ONE*, vol. 4, no. 9, Sep. 2009.

[3] X. D. Liu and D. E. Kourennyi, “Effects of tetraethylammonium on Kx channels and simulated light response in rod photoreceptorss,” *Annals of biomedical engineering*, vol. 32, no. 10, pp. 1428–1442, 2004.

[4] B. Dreher and S. R. Robinson, *Neuroanatomy of the visual pathways and their development*. CRC Press, 1991.

[5] Y. Kamiyama, T. O’Sura, and S. Usui, “Ionic current model of the vertebrate rod photoreceptor,” *Vision research*, vol. 36, no. 24, pp. 4059–4068, 1996.

[6] G. D. Field et al., “Functional connectivity in the retina at the resolution of photoreceptors,” *Nature*, vol. 467, no. 7316, pp. 673-677, Oct. 2010.

[7] D. Attwell, M. Wilson, and S. M. Wu, “A quantitative analysis of interactions between photoreceptors in the salamander (Ambystoma) retina.,” *The Journal of physiology*, vol. 352, no. 1, p. 703, 1984.

[8] J. Dowling, “Retina,” *Scholarpedia*, vol. 2, no. 12, p. 3487, 2007.

Appendix 1 taken from Scholarpedia article [8]